Choreographing Oscillatory Hydrodynamics with DNA-Coated Gold Nanoparticles

Anish Rao,*,† Ana Sánchez Iglesias,† and Marek Grzelczak*,†,‡

†*Centro de Física de Materiales CSIC-UPV/EHU, Paseo Manuel de Lardizabal 5, 20018 Donostia San-Sebastián, Spain*

‡*Donostia International Physics Center (DIPC), Paseo Manuel de Lardizabal 4, 20018 Donostia-San Sebastián, Spain*

Received May 7, 2024; E-mail: anish.rao@ehu.eus; marek.g@csic.es

Abstract: Periodic responses to non-periodic energy inputs are hallmarks of living systems, that lead to metastable features across length scales, exemplified by phenomena such as oscillations. Experimental attempts to mimic such phenomenon have primarily utilized (macro)molecular building blocks that enable precise control over interactions and thus hierarchical design. Nanoparticle-based systems have largely remained unexplored in the generation of oscillatory features. In this study, we propose a nanosystem featuring hierarchical response to light energy input where the subtle interplay of thermoplasmonic effects and reversible surface chemistry of DNA-based ligands render oscillatory hydrodynamic flows. The slow aggregation of gold nanoparticles (AuNPs) serves as a positive feedback loop, while fast photothermal disassembly acts as the negative feedback. These asymmetric feedback loops, combined with thermal hysteresis as time delay mechanism, are essential ingredients for orchestrating an oscillating response. Our findings contribute to the advancement of oscillating systems, thereby paving the way for the development of next-generation dynamic materials.

Successful preparation of self-assembled systems has long been recognized as a significant achievement in its own right.[1–3] Inspired by nature's ingenuity, researchers have devoted efforts to understanding and mimicking naturally occurring self-assembled structures and functions to systems composed of non-biological components.[4] This has rendered remarkable developments in regulating interparticle interactions and controlling the spatial arrangement of building blocks to form a wide variety of static[1,2,5] and dynamic self-assemblies.[3,6,7] Dynamic assemblies can be moulded into diverse states under suitable external stimuli, exhibiting switchable,[8–10] transient,[11] or oscillating[12] behaviour. Particularly attractive is the design of systems demonstrating periodic responses under non-periodic energy supply, i.e. *self-oscillations*[13] since they have been envisaged to outperform their steady-state counterparts, especially in the context of catalytic applications.[14] Despite recent advancements in this domain,[12,15–20] designing functional and modular self-oscillators presents a formidable challenge — one that holds immense potential for advancing various fields.

Traditionally, chemical oscillations were achieved using organic and inorganic reagents in continuous stirred tank reactors and flows[21,22] or enzymatic networks.[23] The key design components include an interplay between *positive* and *negative* feedback loops separated by a *time delay*.[24] Although the above-mentioned oscillating responses have been exploited to induce similar patterns in colloids,[25] polymers,[26] or gels,[27] the macroscopic manifestation of oscillatory patterns - detectable by the naked eye - seems to be reserved only for molecular systems. The central hypothesis of the present work states that hierarchical design of nanoparticles-based systems in which thermoresponsive surface ligands regulate the reversible clustering of nanoparticles under uninterrupted light conditions can eventually generate oscillatory signatures driven by hydrodynamic convection (Figure 1).

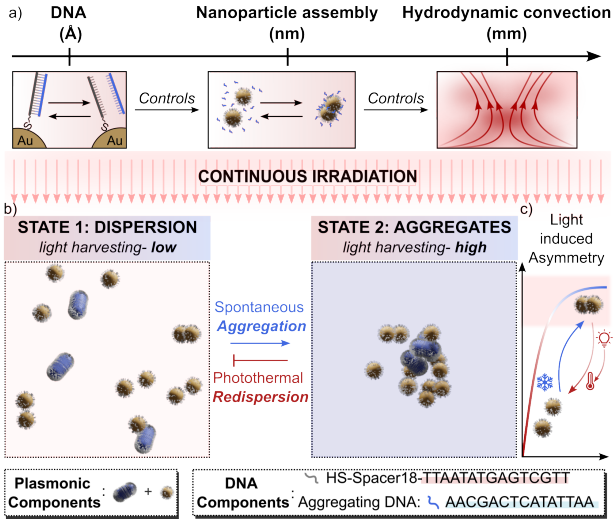

Figure 1. Schematic diagram of proposed oscillatory nanosystem. a) Hierarchical design of the system in which thermo-sensitive hybridization of DNA surface ligands (molecular scale) controls reversible assembly of nanoparticles (nanoscale) that in turn set the initial conditions for oscillatory convection upon disassembly on macro scale. b) Feedback mechanism. Under non-periodic light conditions at NIR, the binary mixture of gold spheres and rods show minimal light-harvesting capabilities and undergoes spontaneous assembly through DNA hybridization (positive feedback). Upon successful assembly, the system eventually harvests enough light energy at NIR to initiate photothermal disassembly (negative feedback). The oscillatory features emerge from light-induced asymmetry (shown in c), wherein preferential interaction of assemblies with light accelerates their own disassembly.

Specifically, we selected DNA-triggered spontaneous and non-specific aggregation of AuNPs as the *positive feedback* and their heat-induced redispersion as the *negative feedback* mechanism (Figure 1). Here, the aggregation-induced redshift in the extinction of AuNPs increases the light-harvesting properties of the system in the assembled state under non-periodic irradiation with a laser that serves as the energy source. This increased light absorption produces photothermal heating that results in the melting of DNA and ultimately, the disassembly of AuNPs (*light-induced*

asymmetry, see Figure 1c). The *time delay* was introduced through thermal hysteresis which is a typical feature of self-assembling NP.[28,29] Under suitable experimental conditions (base temperature and laser power), we observed that the local heating by AuNPs, coupled with thermoresponsive self-assembly could induce forces (*thermal buoyancy*)[30] that resulted in hydrodynamic oscillations in our system. Although the oscillations could be observed for a range of temperatures and laser powers, they were sensitive to the initial conditions of the experiment. Our system thus exhibits hierarchical features, where, angstrom scale molecular components control the assembly of NPs, which finally translates into mm-scale oscillating hydrodynamic flows (Figure 1a). These oscillating hydrodynamic flows have potential applications in the fields of chemical computing, fuzzy logic, and artificial neuron network models.[31–33]

To assure the increase of extinction at the NIR spectral range (∼808 nm, resonant with the laser light source) we selected a mixture of DNA-coated gold nanospheres (AuSs, diameter = 28.2 ± 2.4 nm, Figure S1) and gold nanorods (AuNRs, length = 54.5 ± 4.8 nm, width = 18.6 ± 1.5 nm, Figure S2). The native ligands were place exchanged with thiolated DNA (see Figure 1) using the freeze-drying method.[34] For more details on the synthesis and ligand exchange process, see Section S1.2, and S1.3 in the SI. These DNA-coated AuNPs underwent aggregation in the presence of complementary DNA (aggregating DNA) under high ionic strength (∼200mM NaCl) due to the *salting-out* effect (Figure 2b).[35] Note that unary systems based on either AuSs or AuNRs were unable to exhibit the desired spectral shift upon aggregation. Although a dispersion of AuSs exhibits redshifts during aggregation, their photothermal heating is relatively poor (weak negative feedback) (see Figure S4, S5).[36] Conversely, AuNRs despite having high photothermal heating abilities, often display minor redshifts due to more stable side-to-side assembly configurations (see Figure S6).[5] By mixing and assembling AuNRs and AuSs, unstructured aggregates form that exhibit reliable and consistent redshifts along with high photothermal heating abilities, thereby fulfilling both important criteria for choreographing an oscillating response.

Kinetic asymmetry is an essential ingredient of many biological non-equilibrium systems (e.g., microtubule assembly).[37] Our colloidal system is designed in a way to be sensitive to the external stimulus exclusively in the assembled state (negative feedback). That is, only upon assembly, the system absorbs the irradiated energy source; i.e. continuous wave laser in the NIR spectral range (808 nm) (see Figure S3). At the laser wavelength, the incoming light is detuned from the plasmonic responses of both components (∼523 nm for AuSs, ∼685 nm for AuNRs) in their dispersed state, thereby minimizing its interaction with the stimulus. Only upon the assembly of the NP mixture, a redshift occurs, increasing the absorbance at 808 nm (Figures 2b, c). The rate of aggregation was estimated to be 0.17 min^{-1}. The unstructured nature of the assembly is further evident in the transmission electron microscopy images shown in Figure 2d. Upon aggregation, the extinction at the laser wavelength (1.9 W) progressively increases that triggers photothermal heating and thus melting dsDNA to ultimately initiate disintegration of assemblies within 2 minutes (see red curve in Figure 2c). Under these conditions, the rate of redispersion was 10.68 min^{-1}, considerably higher than the rate of aggregation. Notably, the assembly-disassembly cycles were successfully performed a minimum of 15 times, as shown in Figure 2e and S7, demonstrating high repeatability and minimum losses. Here, the assembly was performed by exposing the AuNP dispersion containing complementary DNA to a temperature of 15°C (shown in blue in Figure 2e), while disassembly was conducted using 808 nm laser with a power of 1.9 W (shown in red in Figure 2e).

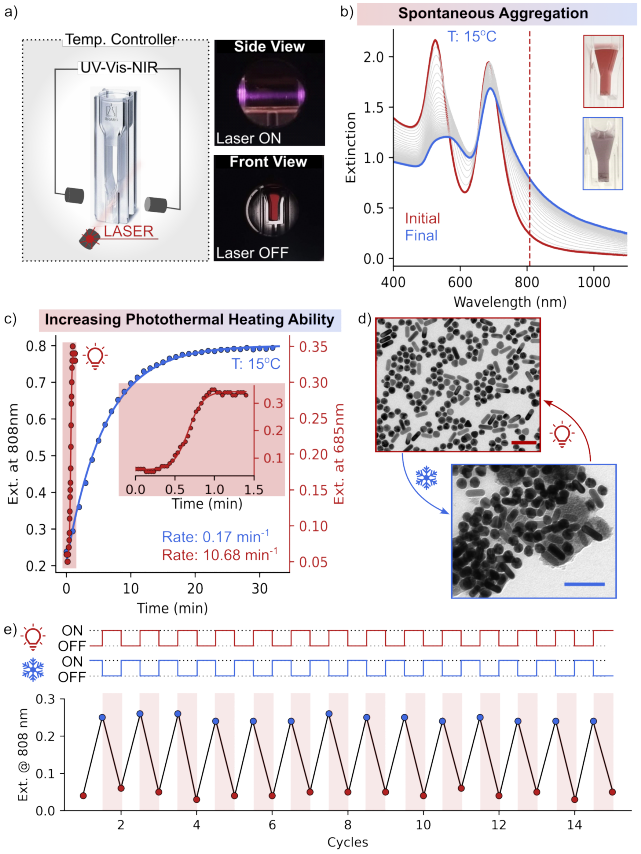

Figure 2. Positive and negative feedback through reversible assembly a) Schematic diagram of the experimental setup in which light energy (CW laser at 808 nm) is delivered orthogonal to UV-Vis-NIR spectral probe. Optical images showing both the front and side views of the cuvette containing AuNPs in the temperature controller. The side view shows the path of the laser during the irradiation. b) Time-dependent UV-Vis-NIR spectra of the binary AuNP mixture during assembly. Here, the system shows a consistent redshift and a simultaneous decrease in the extinction intensity due to non-specific plasmon coupling. Optical images showing the initial and final states during the assembly are shown in the inset. c) The increase in the extinction intensity at 808 nm (tuned to laser irradiation) during the course of aggregation. d) TEM images of the disassembled and assembled nanoparticles. Scale bar = 100 nm. e) A series of 15 cycles showing temperature-induced assembly (shown in blue), and light-induced disassembly (shown in red) of the system.

A delay in the system's response to an external stimulus is critical for obtaining oscillating features, which allows for avoiding monotonous steady states.[24] Although different strategies can be employed to introduce a time delay, hysteresis is one attractive methodology.[24] To evaluate the presence of thermal hysteresis in our system, we conducted reversible assembly under a temperature ramp of 0.5°C/min, spanning from 10 to 40°C (Figure 3a). We observed a freezing temperature (T_f) of 14.4°C and a melting temperature (T_m) of 22.4°C under dark conditions. Interestingly, these temperatures were shifted under laser conditions. Specifically, as laser power increased, both the freezing and melt-

ing temperatures decreased (see Figure 3b). Although these shifts are small, analysis performed by following the extinction at 523 nm (corresponding to AuSs) also shows a similar trend of decreasing transition temperatures. These shifts are attributed to the photothermal heat generated by the NPs under laser irradiation. With the presence of additional photothermal heat, more amount of heat needs to be *taken away* from the system to assemble the NPs, thereby decreasing the freezing temperature. Conversely, less heat needs to be *supplied* to disassemble the NPs, leading to a decrease in the melting temperature as well. For a detailed discussion on the effect of photothermal heating on transition temperatures, see Figure S8 in the SI. It is noteworthy that at a laser power of ∼135 mW, the system failed to assemble even at 10°C, that is due to the excessive photothermal heating, emphasizing the critical role of laser power in modulating assembly-disassembly dynamics.

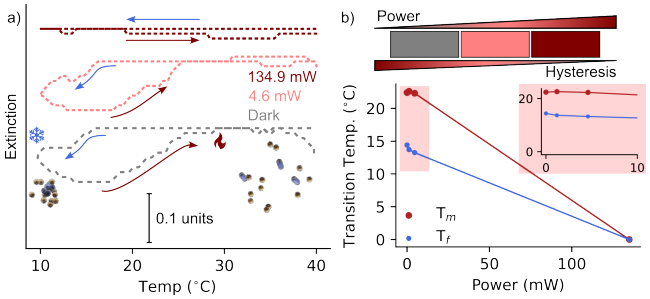

Figure 3. Time delay through thermal hysteresis a) Variation in the hysteresis of the system with increasing laser powers. Here, thermal hysteresis of the system was followed using extinction at wavelengths ∼685 nm within a temperature range spanning 10°C to 40°C, at a scan rate of 0.5°C/min. Arrows indicate the direction of the temperature ramp. b) Schematic showing the qualitative effect of increasing laser power on the hysteresis present in the system. At low laser powers, the system exhibits hysteresis (grey box), which diminishes as the laser power increases (red box). The graph shows the variation of transition temperatures during heating (T_m, red) and cooling (T_f, blue) versus laser power. The inset shows the variations in transition temperatures at low laser powers.

With all the feedback mechanisms in place, we investigated the conditions for observing the onset of oscillations. As an initial state, we set a completely precipitated AuNP mixture on the bottom of the cuvette. The solution was irradiated with a CW 808 nm laser with a beam a few mm above the precipitates and with UV-Vis-NIR probe volume located orthogonal to the laser beam. The spectra were recorded at intervals of 2s for 2 hours (Figure 2a). Under low laser power (∼4.6 mW), NPs remained aggregated since insufficient energy was provided to induce photothermal effects, that is, the extinction at LSPR remained unchanged (Figure 4a - black line). Under high laser power (∼562.5 mW), we observed monotonic redispersion of NPs (Figure 4a - red line). Intriguingly, at laser powers adequate for redispersion, but overwhelming the aggregation of AuNPs (∼134.9 mW), the extinction value at 685 nm exhibited oscillatory dynamics (Figure 4a - blue line). The amplitude of oscillations ΔExt. was ∼0.02. The oscillating response was further analyzed using Fourier analysis, revealing the major component of oscillation corresponding to a period of 0.028 Hz, or a frequency of ∼36 s (Figure 4b, c). These oscillating traces are sensitive to initial and environmental conditions like base temperature and light power.

The oscillations were also observed under alternative conditions, such as at 17°C at ∼134.9, and ∼299.5 mW (see Figure 4d). At lower laser powers, the system remained at stationary state, while with increasing laser powers oscillatory response appeared. Interestingly, we observed increasing frequencies with increasing laser power, with the major oscillating frequency increasing from ∼71 s (0.014 Hz) to ∼166 s (0.006 Hz) while increasing the laser power from ∼134.9 mW to ∼299.5 mW at a base temperature of 17°C.

We postulate that the oscillations originate from temperature-dependent changes in the buoyancy of the dispersion, leading to organized convective flows. We observed oscillations in the extinction intensity at ∼523 nm corresponding to the extinction of AuSs (see Figure S9). This observation hints at the possibility of the oscillations originating from hydrodynamic flows, changing the amount of NPs in the UV-Vis-NIR probe volume. Notably, we observed a coloured chemical hydrodynamic wave-like pattern in the solution, providing additional evidence for the hydrodynamic origins of the oscillations (see the optical image in Figure 4c). This hydrodynamic wave-like pattern is produced by the convective motion of the solvent dragging with itself, the NP mixture. Similar flow-based oscillations have been shown in the literature,[31] but they require higher sample volume and a need for a volatile solvent to establish a strong enough temperature gradient for observing oscillations. The distinct benefit of using plasmonic NPs is their ability to establish potent enough temperature gradients even at 200 μL solutions, compared to 3 mL volumes required in earlier pioneering works.[31]

To induce oscillation, the following critical parameters were established: temperature gradient, thermoresponsiveness and feedback loop asymmetry. We confirmed these parameters through a series of negative control experiments which led to stationary, non-oscillatory responses. First, no oscillation was observed for CTAB-coated AuNRs instead of DNA (see Figure S11). Second, the use of unary building blocks either AuSs or AuNRs generated a stationary state that was attributed to poor photothermal heating (in the case of AuSs) (Figure S4), or negligible redshifts in the extinction spectrum upon assembly (in the case of AuNRs) (Figure S6). Third, using a laser wavelength of 670 nm failed to generate oscillatory dynamics that is due to its inability to induce asymmetry in the system since both unassembled and assembled states possess similar extinction. These experiments underscore and reiterate the critical need for thermoresponsive assembly, as well as the significant increase in extinction at the laser illumination during the assembly, as essential components for obtaining the oscillating response. Finally, we ruled out the contribution of reversible assembly/disassembly of NPs to oscillatory features. The LSPR shift is a signature of decreased interparticle distance that increases plasmon coupling and thereby controls the photothermal effect. In the present case, the LSPR shifts at the λ_{max} was negligible throughout the oscillations (see Figure S10).

Typically, oscillations by nature are highly dynamic and non-linear and thus sensitive to the initial conditions.[38] We performed multiple control experiments ranging from a completely unassembled state (see Figure S12) to aggregated dispersion of AuNPs (see Figure S13), observing that only upon starting the assembly from the completely precipitated dispersion of the AuNP one can observe hydrodynamic oscillations.

In summary, our study shows the design principles involved in the development of NP-based oscillators and ex-

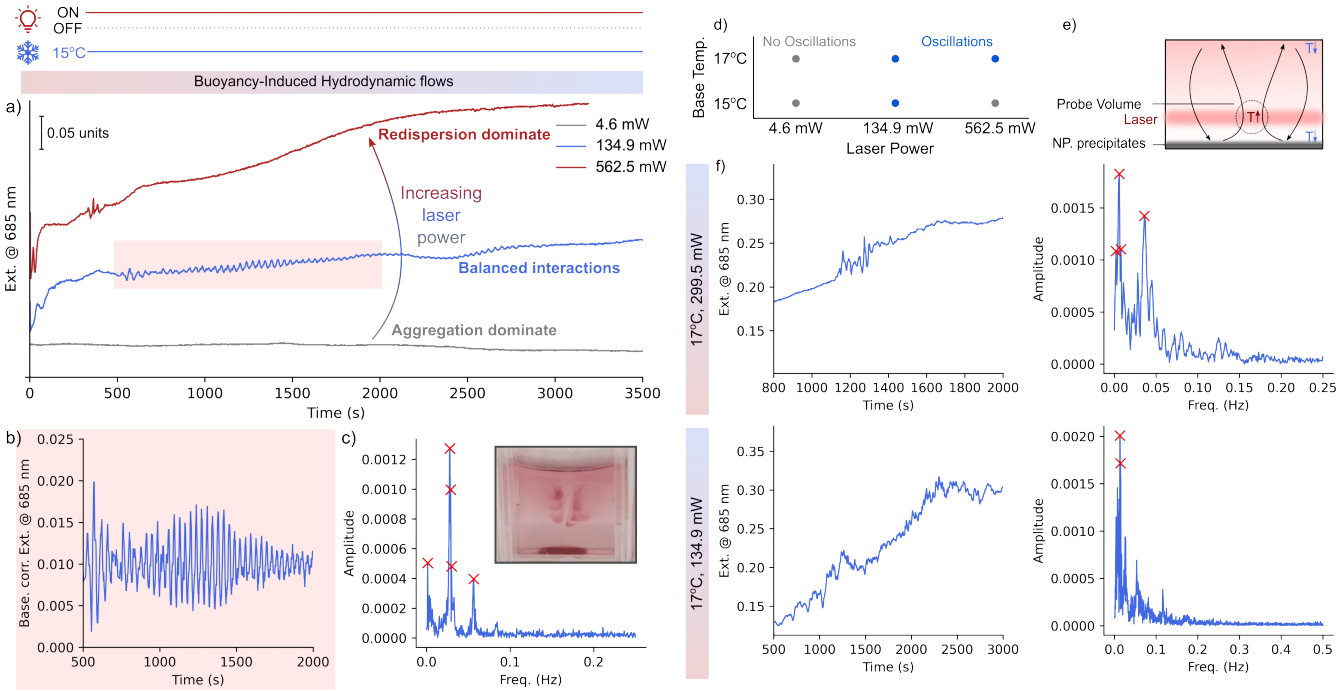

Figure 4. Oscillatory hydrodynamic flows a) Extinction response of the system (15°C, ∼134.9 mW) showing oscillatory signature. b,c) Zoomed UV-Vis-NIR trace (500s - 1000s, highlighted in pink)and corresponding Fourier analysis. Inset in c): digital image showing a coloured chemical hydrodynamic wave-like pattern within the cuvette. d) The phase space represents the interplay between base temperature (which governs aggregation) and laser power (which controls the redispersion of the AuNP mixture). Conditions that show oscillating responses are highlighted in blue. e) Schematic illustrating the origin of hydrodynamic oscillations through temperature difference-induced organized flows within our system. f) UV-Vis-NIR trace showing the oscillating extinction response, and corresponding Fourier analysis of the system at 17°C and a laser power of ∼299.5 and ∼134.9 mW.

tends beyond the conventional approach of regarding self-assemblies as static end products, instead aiming to use them as starting points to generate dynamic states. We systematically employ a combination of DNA-coated AuNPs that exhibit temperature-dependent self-assembly behaviour, coupled with the ability of photothermal heating to induce an oscillating response. Our design ensures that the self-assembled state can preferentially interact with the laser, thereby showing asymmetry which is recognized as a crucial feature in non-equilibrium systems. We foresee coupling the oscillating response to NP catalysis and amplifying the oscillating response. Also, our results open up the possibilities for constructing larger and finely tuned reaction cycles to achieve oscillating self-assemblies. Finally, our study positions AuNPs as compelling and attractive models for studying non-equilibrium systems and usher the realization of exciting properties under non-equilibrium conditions.

Acknowledgement A.R. acknowledges funding from the Spanish MICIU for the Juan de la Cierva (FJC2021-047710-I) fellowship. M.G. acknowledges the grant PID2022-141017OB-I00 funded by MCIN/AEI/10.13039/501100011033 and by "ERDF A way of making Europe". The authors acknowledge the financial support received from the IKUR Strategy under the collaboration agreement between the Ikerbasque Foundation and Materials Physics Center on behalf of the Department of Education of the Basque Government.

Supporting Information Available

Synthesis details and ligand exchange protocol for AuNRs and AuSs; schematic demonstrating the experimental setup; UV–vis–NIR, TEM measurements for AuSs and AuNR, and control experiments. The references that are included in the supporting information are[34,39–41]

References

(1) Boles, M. A.; Engel, M.; Talapin, D. V. Self-assembly of colloidal nanocrystals: From intricate structures to functional materials. *Chem. Rev.* **2016**, *116*, 11220–11289.
(2) Rao, A.; Roy, S.; Jain, V.; Pillai, P. P. Nanoparticle self-assembly: from design principles to complex matter to functional materials. *ACS Appl. Mater. Interfaces* **2022**, *15*, 25248–25274.
(3) Whitesides, G. M.; Grzybowski, B. Self-assembly at all scales. *Science* **2002**, *295*, 2418–2421.
(4) Liu, A. T.; Hempel, M.; Yang, J. F.; Brooks, A. M.; Pervan, A.; Koman, V. B.; Zhang, G.; Kozawa, D.; Yang, S.; Goldman, D. I.; others Colloidal robotics. *Nat. Mater.* **2023**, *22*, 1453–1462.
(5) Bishop, K. J.; Wilmer, C. E.; Soh, S.; Grzybowski, B. A. Nanoscale forces and their uses in self-assembly. *Small* **2009**, *5*, 1600–1630.
(6) Whitesides, G. M.; Ismagilov, R. F. Complexity in chemistry. *science* **1999**, *284*, 89–92.
(7) Grzelczak, M. Colloidal systems chemistry. Replication, reproduction and selection at nanoscale. *J Colloid Interface Sci* **2019**, *537*, 269–279.
(8) Grzelczak, M.; Liz-Marzán, L. M.; Klajn, R. Stimuli-responsive self-assembly of nanoparticles. *Chem. Soc. Rev.* **2019**, *48*, 1342–1361.
(9) Sánchez-Iglesias, A.; Claes, N.; Solís, D. M.; Taboada, J. M.; Bals, S.; Liz-Marzán, L. M.; Grzelczak, M. Reversible clustering of gold nanoparticles under confinement. *Angew. Chemie.* **2018**, *130*, 3237–3240.
(10) Rao, A.; Roy, S.; Unnikrishnan, M.; Bhosale, S. S.; Devatha, G.; Pillai, P. P. Regulation of interparticle forces reveals controlled aggregation in charged nanoparticles. *Chem. Mater.* **2016**, *28*, 2348–2355.

(11) Rao, A.; Roy, S.; Pillai, P. P. Temporal Changes in Interparticle Interactions Drive the Formation of Transiently Stable Nanoparticle Precipitates. *Langmuir* **2021**, *37*, 1843–1849.
(12) Mezzasalma, S. A.; Kruse, J.; Merkens, S.; Lopez, E.; Seifert, A.; Morandotti, R.; Grzelczak, M. Light-Driven Self-Oscillation of Thermoplasmonic Nanocolloids. *Adv. Mater.* **2023**, *35*, 2302987.
(13) Shen, B.; Kang, S. H. Designing self-oscillating matter. *Matter* **2021**, *4*, 766–769.
(14) Ardagh, M. A.; Birol, T.; Zhang, Q.; Abdelrahman, O. A.; Dauenhauer, P. J. Catalytic resonance theory: superVolcanoes, catalytic molecular pumps, and oscillatory steady state. *Catal. Sci. Technol.* **2019**, *9*, 5058–5076.
(15) Howlett, M. G.; Engwerda, A. H.; Scanes, R. J.; Fletcher, S. P. An autonomously oscillating supramolecular self-replicator. *Nature Chemistry* **2022**, *14*, 805–810.
(16) Zhang, H.; Zeng, H.; Eklund, A.; Guo, H.; Priimagi, A.; Ikkala, O. Feedback-controlled hydrogels with homeostatic oscillations and dissipative signal transduction. *Nat. Nanotechnol.* **2022**, *17*, 1303–1310.
(17) Pogodaev, A. A.; Wong, A. S.; Huck, W. T. Photochemical control over oscillations in chemical reaction networks. *J. Am. Chem. Soc.* **2017**, *139*, 15296–15299.
(18) Leira-Iglesias, J.; Tassoni, A.; Adachi, T.; Stich, M.; Hermans, T. M. Oscillations, travelling fronts and patterns in a supramolecular system. *Nat. Nanotechnol.* **2018**, *13*, 1021–1027.
(19) Altemose, A.; Sánchez-Farrán, M. A.; Duan, W.; Schulz, S.; Borhan, A.; Crespi, V. H.; Sen, A. Chemically controlled spatiotemporal oscillations of colloidal assemblies. *Angew. Chem. Int. Ed.* **2017**, *56*, 7817–7821.
(20) Shklyaev, O. E.; Balazs, A. C. Lifelike behavior of chemically oscillating mobile capsules. *Matter* **2022**, *5*, 3464–3484.
(21) Semenov, S. N.; Kraft, L. J.; Ainla, A.; Zhao, M.; Baghbanzadeh, M.; Campbell, V. E.; Kang, K.; Fox, J. M.; Whitesides, G. M. Autocatalytic, bistable, oscillatory networks of biologically relevant organic reactions. *Nature* **2016**, *537*, 656–660.
(22) Kovacs, K.; McIlwaine, R. E.; Scott, S. K.; Taylor, A. F. pH oscillations and bistability in the methylene glycol–sulfite–gluconolactone reaction. *Phys. Chem. Chem. Phys.* **2007**, *9*, 3711–3716.
(23) Ghosh, S.; Baltussen, M. G.; Ivanov, N. M.; Haije, R.; Jakstaite, M.; Zhou, T.; Huck, W. T. Exploring Emergent Properties in Enzymatic Reaction Networks: Design and Control of Dynamic Functional Systems. *Chem. Rev.* **2024**,
(24) Novák, B.; Tyson, J. J. Design principles of biochemical oscillators. *Nat. Rev. Mol. Cell Biol.* **2008**, *9*, 981–991.
(25) Lagzi, I.; Kowalczyk, B.; Wang, D.; Grzybowski, B. A. Nanoparticle oscillations and fronts. *Angew. Chem. Int. Ed.* **2010**, *49*, 8616–8619.
(26) Yoshida, R.; Ueki, T. Evolution of self-oscillating polymer gels as autonomous polymer systems. *NPG Asia Mater* **2014**, *6*, e107–e107.
(27) Yoshida, R.; Takahashi, T.; Yamaguchi, T.; Ichijo, H. Self-oscillating gel. *J. Am. Chem. Soc.* **1996**, *118*, 5134–5135.
(28) O'Brien, M. N.; Brown, K. A.; Mirkin, C. A. Critical undercooling in DNA-mediated nanoparticle crystallization. *ACS Nano* **2016**, *10*, 1363–1368.
(29) Wang, D.; Kowalczyk, B.; Lagzi, I.; Grzybowski, B. A. Bistability and hysteresis during aggregation of charged nanoparticles. *J. Phys. Chem. Lett.* **2010**, *1*, 1459–1462.
(30) Rayleigh, L. On convection currents in a horizontal layer of fluid, when the higher temperature is on the under side. *Philos. Mag.* **1916**, *32*, 529–546.
(31) Gentili, P. L.; Dolnik, M.; Epstein, I. R. "Photochemical oscillator": colored hydrodynamic oscillations and waves in a photochromic system. *J. Phys. Chem. C* **2014**, *118*, 598–608.
(32) Gentili, P. L. Small steps towards the development of chemical artificial intelligent systems. *RSC Adv.* **2013**, *3*, 25523–25549.
(33) Gorecki, J.; Gizynski, K.; Guzowski, J.; Gorecka, J. N.; Garstecki, P.; Gruenert, G.; Dittrich, P. Chemical computing with reaction–diffusion processes. *Philos. Trans. Math. Phys. Eng. Sci.* **2015**, *373*, 20140219.
(34) Liu, B.; Liu, J. Freezing directed construction of bio/nano interfaces: reagentless conjugation, denser spherical nucleic acids, and better nanoflares. *J. Am. Chem. Soc.* **2017**, *139*, 9471–9474.
(35) Sato, K.; Hosokawa, K.; Maeda, M. Rapid aggregation of gold nanoparticles induced by non-cross-linking DNA hybridization. *J. Am. Chem. Soc.* **2003**, *125*, 8102–8103.
(36) Qin, Z.; Wang, Y.; Randrianalisoa, J.; Raeesi, V.; Chan, W. C.; Lipiński, W.; Bischof, J. C. Quantitative comparison of photothermal heat generation between gold nanospheres and nanorods. *Sci. Rep.* **2016**, *6*, 29836.
(37) Ragazzon, G.; Prins, L. J. Energy consumption in chemical fuel-driven self-assembly. *Nat. Nanotechnol.* **2018**, *13*, 882–889.
(38) Gentili, P. L.; Giubila, M. S.; Heron, B. M. Processing binary and fuzzy logic by chaotic time series generated by a hydrodynamic photochemical oscillator. *ChemPhysChem* **2017**, *18*, 1831–1841.
(39) Bastús, N. G.; Comenge, J.; Puntes, V. Kinetically controlled seeded growth synthesis of citrate-stabilized gold nanoparticles of up to 200 nm: size focusing versus Ostwald ripening. *Langmuir* **2011**, *27*, 11098–11105.
(40) Vigderman, L.; Zubarev, E. R. High-yield synthesis of gold nanorods with longitudinal SPR peak greater than 1200 nm using hydroquinone as a reducing agent. *Chem. Mater.* **2013**, *25*, 1450–1457.
(41) Mehtala, J. G.; Zemlyanov, D. Y.; Max, J. P.; Kadasala, N.; Zhao, S.; Wei, A. Citrate-stabilized gold nanorods. *Langmuir* **2014**, *30*, 13727–13730.

TOC Graphic